Hindawi
Advances in Condensed Matter Physics
Volume 2018, Article ID 1257543, 8 pages
https://doi.org/10.1155/2018/1257543

Research Article

Optical and Electrical Properties of TiO_2/Co/TiO_2 Multilayer Films Grown by DC Magnetron Sputtering

Marcos G. Valluzzi,[1] Lucas G. Valluzzi,[1] Marcos Meyer,[2] María A. Hernández-Fenollosa,[3] and Laura C. Damonte[2]

[1] *IDEI, Universidad Nacional de Tierra del Fuego (UNTDF), Ushuaia 9410, Argentina*
[2] *Dto. de Física, Facultad de Ciencias Exactas, UNLP-IFLP, CCT, CONICET, La Plata 1900, Argentina*
[3] *Instituto de Tecnología de Materiales, Universitat Politècnica de València, Camino de Vera s/n, Valencia 46022, Spain*

Correspondence should be addressed to Laura C. Damonte; damonte@fisica.unlp.edu.ar

Received 31 January 2018; Accepted 13 May 2018; Published 7 June 2018

Academic Editor: Jörg Fink

Copyright © 2018 Marcos G. Valluzzi et al. This is an open access article distributed under the Creative Commons Attribution License, which permits unrestricted use, distribution, and reproduction in any medium, provided the original work is properly cited.

Transparent oxide multilayer films of TiO_2/Co/TiO_2 were grown on glass substrate by DC magnetron sputtering technique. The optical and electrical properties of these films were analyzed with the aim of substituting ITO substrate in optoelectronic devices. The samples were characterized by UV-visible spectroscopy, atomic force microscopy (AFM), and Kelvin probe force microscopy (KPFM). The effect of Co interlayer thickness (4, 8, and 12 nm) on the transmittance spectra yielded an optical absorption edge shift. The work function of these films was determined by KPFM technique allowing us to predict the Fermi level shift by extending the model for pure materials to our multilayer system. The Fermi level and optical absorption edge seem to be correlated and shifted toward lower energies when Co interlayer thickness is increased.

1. Introduction

Transparent conductive oxides (TCOs) play an important role in many optoelectronic devices, like solar cells, organic light emitting diodes, liquid crystal displays, touch panel, and others technological applications [1–5]. In recent years, Sn-doped indium oxide (ITO) is the material most used in optoelectronic applications due to a high transmittance in the visible spectrum ($\sim 80\,\%$) and a low electrical resistivity ($\sim 10^{-4}\,\Omega$cm) [6]. However, indium is toxic and has limited supply, which restricts its large scale applications. For these reasons, it is crucial to search for cheaper materials with good optoelectrical properties. Recently, many researchers proposed a TCO/metal/TCO multilayer structure with advanced electrical properties, chemical stability, and high optical transparency compared to a TCO single layer. Among others, materials such as Nb_2O_5, AZO (Al doped ZnO), and TiO_2 had been studied for potential ITO substitutes [7–11]. Multilayer films of TiO_2/Ag/TiO_2 and TiO_2/Cu/TiO_2 achieved excellent results [7, 12–14]. Titanium dioxide has been intensively studied over the last decades, because of its wide interesting technological applications, such as solar cells [15], optical coating material [16, 17], and photocatalytic applications [18, 19] as well as a gas sensor [20–24]. Due to its high dielectric constant, TiO_2 thin films have been widely investigated for applications in electronic devices [25]. Recently, magnetic materials doped with transparent conductive oxides to produce a transparent magnetic oxide (TMO) have received considerable attention because of their potential applications in spintronics [26, 27]. In this sense, Co-doped TiO_2 has been a promising candidate [28] because of its physical properties, like ferromagnetic behavior at room temperature, wide-band gap diluted magnetic semiconductors (DMSs), and high Curie temperature [29] among others. However, very few studies over TiO_2/Co/TiO_2 multilayer have been performed [30].

Fermi level is a critical parameter for understanding transport electronic properties, like resistivity, mobility, and so on. Kelvin probe force microscopy (KPFM) is a powerful technique to provide direct evidence on Fermi level energy

[31, 32]. This experimental technique measures the contact potential difference between a conductive atomic tip and the sample (CPD) [33, 34]. KPFM has been extensively used as a unique technique to characterize the nanoscale electric and electronic properties on metal/semiconductors interfaces [35], dopant profiling semiconductor [36], ferroelectrics [37], semiconductors devices [38–41], and surface potential of biomolecules [42, 43]. KPFM is a high lateral resolution technique of approximately 50 nm [44] and is, usually, a two-pass technique; this means that it utilizes two passes to realize the topographical and surface potential scan separately [45, 46].

In the present work, TiO_2/Co/TiO_2 multilayers with different Co interlayer thicknesses are fabricated by DC reactive magnetron sputtering under different atmospheric conditions. The influence of the Co interlayer thickness on the multilayer optical properties is analyzed. Multilayer's Fermi level shift by Kelvin probe force microscopy (KPFM) technique is also determinate and the obtained results were correlated with optical transmission spectra measurements. To our knowledge this is the first time that the consistent linkage between optical band gap and Fermi level energies is shown.

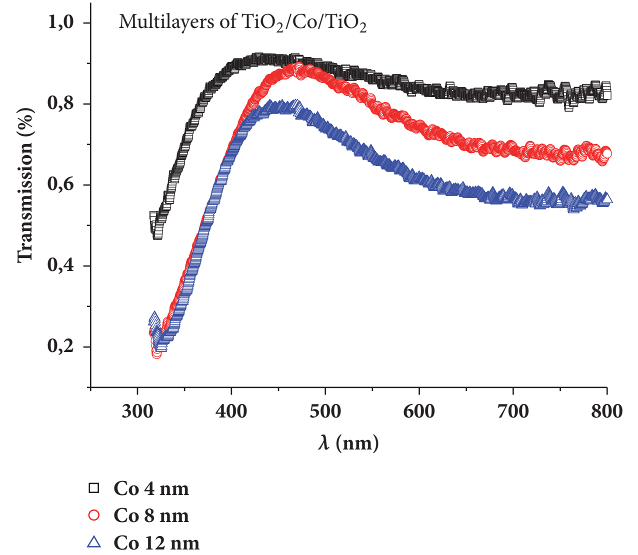

Figure 1: Transmission spectra of multilayers TiO_2/Co/TiO_2 for different Co interlayer thicknesses.

2. Experimental

Multilayer films of $TiO_2/C_O/TiO_2$ of different Co thickness are deposited on commercial glass substrate by DC magnetron co-sputtering deposition system (ATC ORION 8HV AJA International Corporation) using metallic Ti and Co targets (99,99 % purity, 2-inch diameter, 5 mm thickness, ACI alloys Inc). Substrates were ultrasonically cleaned in isopropyl alcohol for ten minutes and dried in nitrogen before deposition. The substrate deposition temperature was 200°C and the working pressure was kept at 10mTorr. Before deposition, the main chamber pressure was $1x10^{-6}$ *Torr*. Target powers were set at 150 W and 100 W for Ti and Co metals, respectively. In order to obtain the bottom and top of TiO_2 layers, the deposition was carried out under a mixture of Ar (99,999%) and O_2 (99,999%) atmosphere with a rate flux of [Ar]/[O_2]=22 sccm/3 sccm (standard cubic centimeters per minute). For the Co intermediate layers a pure Ar atmosphere was established. These conditions yield deposition rates of 0,22 nm/s and 0,3 nm/s for Ti and Co metals, respectively. The deposition time was chosen to obtain an estimated thickness for TiO_2 layers of 30 nm while Co interlayers of 4, 8, and 12 nm thickness were grown. Hereafter, the resulting multilayers will be named S1, S2, and S3, respectively.

Optical transmission characterization was also performed at room temperature with a *Hamamatsu L2175* UV–VIS spectrophotometer in the 300 to 850 nm wavelength range (*Xe* lamp 150 W).

Surface voltage measurements were done with the Kelvin Force probe (KPFM) using a NT-MDT atomic force microscope (AFM) in atmospheric conditions. A Si (n-type) cantilever coated with P_t/I_r (APP NANO) was used. The probe operates at a resonant frequency of 300 KHz, Q factor of 280, and a spring constant k of 40N/m. Surface topography was determinate in the first pass in the semicontact mode, while, in the second pass, the probe was lifted above the surface at the height 30 nm. Surface voltage measured by Kelvin probe is commonly referred to as the contact potential difference voltage, V_{CP}.

3. Results and Discussion

Figure 1 shows the optical transmittance spectra for the three samples S1, S2, and S3 in the wavelength range 300-800 nm. The obtained spectra display a typical behavior with a well defined absorption band edge. In this part of the spectrum, metal-free electrons reflectivity is very small and is affected by light absorption from interband electronic transitions [47]. As Co thickness interlayer increases, more bound electrons are available for excitation producing a decrease in transmittance. Instead, in the long wavelengths, region-free electron reflectivity is high [48] and the optical transmittance diminution with Co thickness is explained by the simple classical Drude model.

The absorption coefficient α can be determined by the equation $\alpha = (1/t)\ln(1/T)$, where t is the film thickness and T is the optical transmittance.

The average transmittance T_{av} for S1, S2, and S3 multilayer film results is 86 %, 80 %, and 67,5 %, respectively. A transmittance diminution with metal interlayer increasing thickness was also observed by Yang. et al. in TiO_2/metal multilayers grown by RF magnetron sputtering [30]. The band gap E_g can be derived from the well known Tauc's expression [49, 50].

$$\alpha h\nu = A\left(h\nu - E_g\right)^m, \quad (1)$$

where m is 1/2 or 2 for allowed direct and indirect electronic transition, respectively. For forbidden direct and indirect transitions m is 3/2 and 3, respectively. Thus, for our system, m=2 value corresponds with an indirect allowed electronic transition. A is a constant and $h\nu$ is the photon energy.

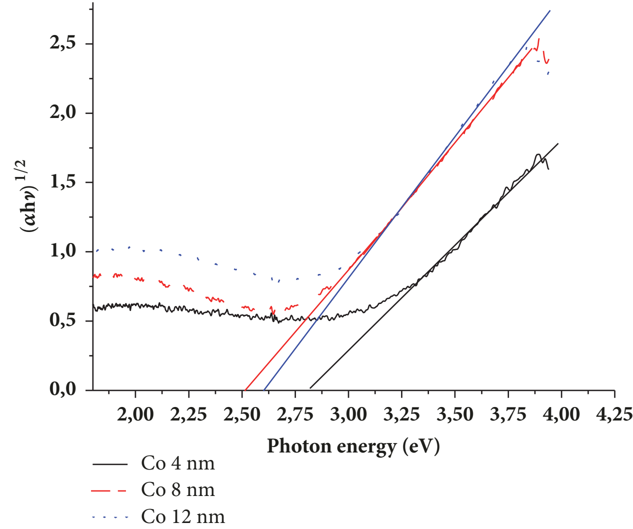

Figure 2: Optical bandgap TiO_2/Co/TiO_2 multilayers. Plot of $(-\ln T \times h\nu)^2$ versus photon energy.

The band gap value can be obtained by extrapolating the linear portion to the photon energy axis ($\alpha h\nu = 0$), as shown in Figure 2. Thus, the obtained band gaps for S1, S2, and S3 samples were 2,8 eV, 2,6 eV, and 2,64 eV, respectively. The total band gap shift was 0,2 eV approximately. Yang et al. [30] reported similar energy band gaps shifts for TiO_2/Co/TiO_2 multilayers with 80 nm TiO_2 layers thickness and Co ultrathin interlayers (<4 nm) obtained by RF magnetron sputtering technique. Other authors [51, 52] also reported a band gap narrowing for M-doped TiO_2 nanoparticles (M: Cu, Ni, and Cr) grown by sol gel method.

In a degenerate semiconductor, such as TiO_2 anatase, the energy band gaps represent the shift in Fermi level. It can be easily shown [51] that the relationship between the work function,∅, and the Fermi level energy, E_F, results:

$$\emptyset = E_{vac} - E_F \tag{2}$$

As already stated, KPFM is a suitable technique to probe the local contact potential difference at a film surface. Since the attractive force between tip and sample is related to the potential drop in the tip-sample junction, the V_{CP} can be determined by adjusting the applied bias voltage.

Figure 3 shows 3D AFM surface topography 10 x10 μm^2 for S1, S2, and S3 samples, respectively. Average roughness analyses were carried out by NOVA software and the following values: 2,72 nm, 2,5 nm, and 1,46 nm, results for S1, S2, and S3, samples, respectively. Henceforth, as the Co interlayer thickness increases, average roughness decreases.

The surface roughness of TCO film plays an important role in determining the optical and electrical properties of the multilayer films; smoother films will have less scattering and hence superior mobility and better transparency. In the present work, optical properties are not only influenced by surface roughness but also by the metal interlayer thickness.

Figure 4 shows KPFM topography and contact potential CP histogram acquired at a distance of 30 nm with an Ac voltage of 3V between the surface and the cantilever during the second pass.

The CP histograms, shown in Figure 5, were analyzed by NOVA software using a Lorentzian function. The obtained contact potential average peaks were −80 mV, −260 mV, and -227 mV for samples S1, S2, and S3, respectively, with Full Width at Half Maximum (FWHM) of 0,06 − 0,09 V for all samples. An appreciable shifting to negative potential is observed as Co thickness increases (Figure 6).

It is well known that in semiconductors the work function depends on the dopant types and their concentrations. In addition, the contact potential of a material can be altered significantly by stray capacitances from the tip geometry [52], tip-sample distance [53], and environment conditions such as the presence of adsorbates, surfaces charges, oxide layers, and water layer on the sample surface [54]. Since the observed differences in both, mean surface roughness and the contact potential, seemed not to be related, it is inferred that the changes in V_{CP} come up from the intrinsic characteristic of the film.

From these results it is possible to estimate the difference in Fermi level energy between two different samples. The contact potential V_{CP} between the sample and AFM tip is defined as follows [39, 55, 56]:

$$V_{CP} = \frac{\emptyset_{sample} - \emptyset_{tip}}{e}, \tag{3}$$

where e is the elementary charge and $\emptyset_{sample}$, $\emptyset_{tip}$ are the work functions of the sample and tip, respectively.

Extending the model for pure materials [31, 55] to our multilayer system the Fermi level shift, ΔE_F , between two samples can be estimated from

$$\Delta E_F = e\left(V_{CPsample1} - V_{CPsample2}\right) \tag{4}$$

Then, the Fermi level shift between S1 and S2 samples was −0,18 eV and -0,15 eV between S1 and S3 with an experimental error of 0,06 eV.

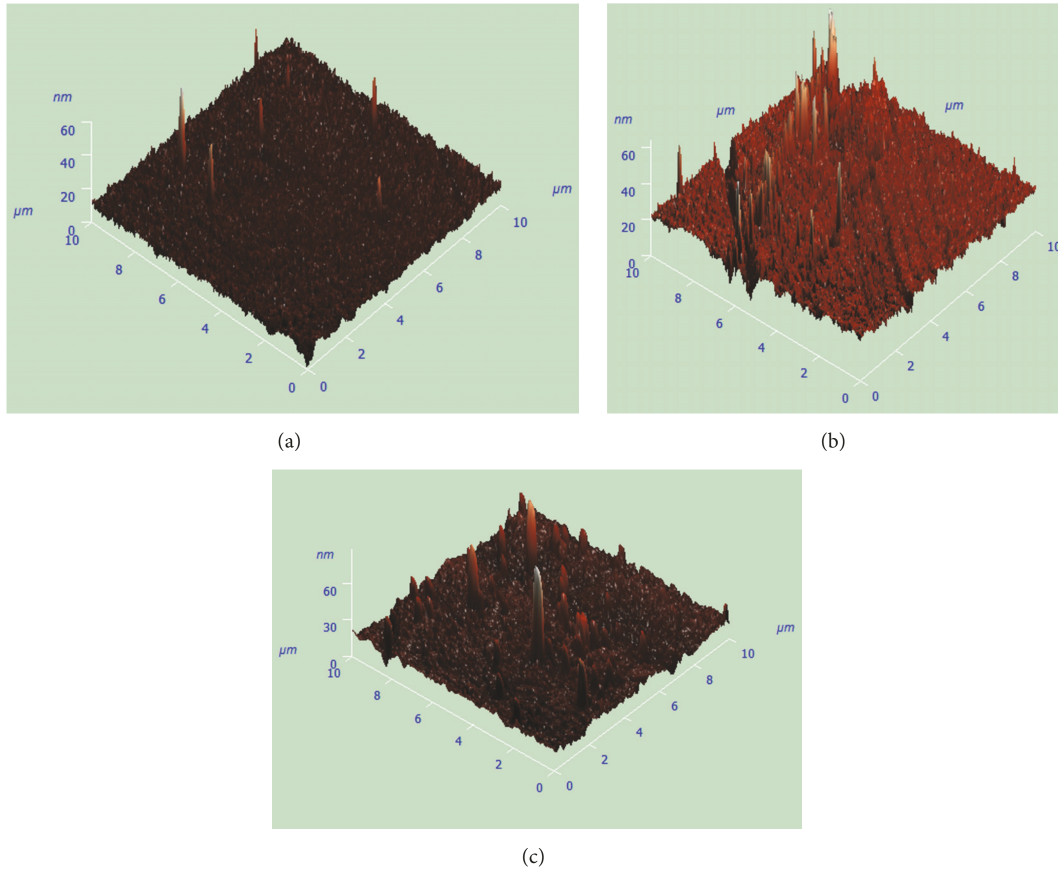

(a)

(b)

(c)

Figure 3: 3D AFM topographical images of $TiO_2/Co/TiO_2$: (a) Co, 4 nm, (b) Co, 8 nm, and (c) Co, 12 nm.

As was already pointed out, since the Fermi energy level in semiconductors depends on doping concentration, the prepared multilayer systems behave as a doped semiconductor. The observed changes in Fermi energy level match up the resulting shifts in band gap energy from optical measurements.

It is worthwhile to note that the KPFM measurements conducted in this study have been made in air, so the obtained values are rather qualitative [57]. However, they are very useful since they provided a fast and cheaper characterization of the samples involved. In addition, since the surface potential itself is always a relative value based on the local CPD between the AFM tip and the sample surface [58], the observed trend is a relative behavior between the studied samples. The changes observed between the films are attributed to the increasing metal intermediate layer and not to sample surface contamination or degradation tip. New experiments with different interlayer metals and thickness are now in course to analyze the effect of an additional charge transfer and the origin of the observed behavior.

4. Conclusions

Summarizing, $TiO_2/Co/TiO_2$ multilayers with different interlayer thickness were fabricated by DC reactive magnetron sputtering under different atmospheric conditions. Band gap shifts of 0,2 eV were found out by optical spectroscopy with respect to S1 sample.

Kelvin probe force microscopy was used to measure the work function of multilayer thin films. The observed variation in the work function with metal interlayer thickness can be related to a concomitant change in the Fermi level by extending the model for pure materials. In consequence, a Fermi level shift of 0,15 eV-0,18 eV from S2 and S3 samples to S1 sample was achieved.

To our knowledge this is the first time the results inferred by this technique were compared with optical data measurements in these multilayer systems revealing a qualitative agreement.

Finally, KPFM emerged as a powerful local technique to determine, in ambient conditions and in a fast way, the work functions of multilayer systems. Fermi level shift of a multilayer system constitutes a potential characterization technique to optoelectronic materials such as transparent conductive oxide (TCO) and transparent magnetic oxide (TMO). A deeper study of the effect of metal interlayer thicknesses on the work function and its relationship with Fermi energy level is in progress.

Data Availability

The data used to support the findings of this study are available from the corresponding author upon request.

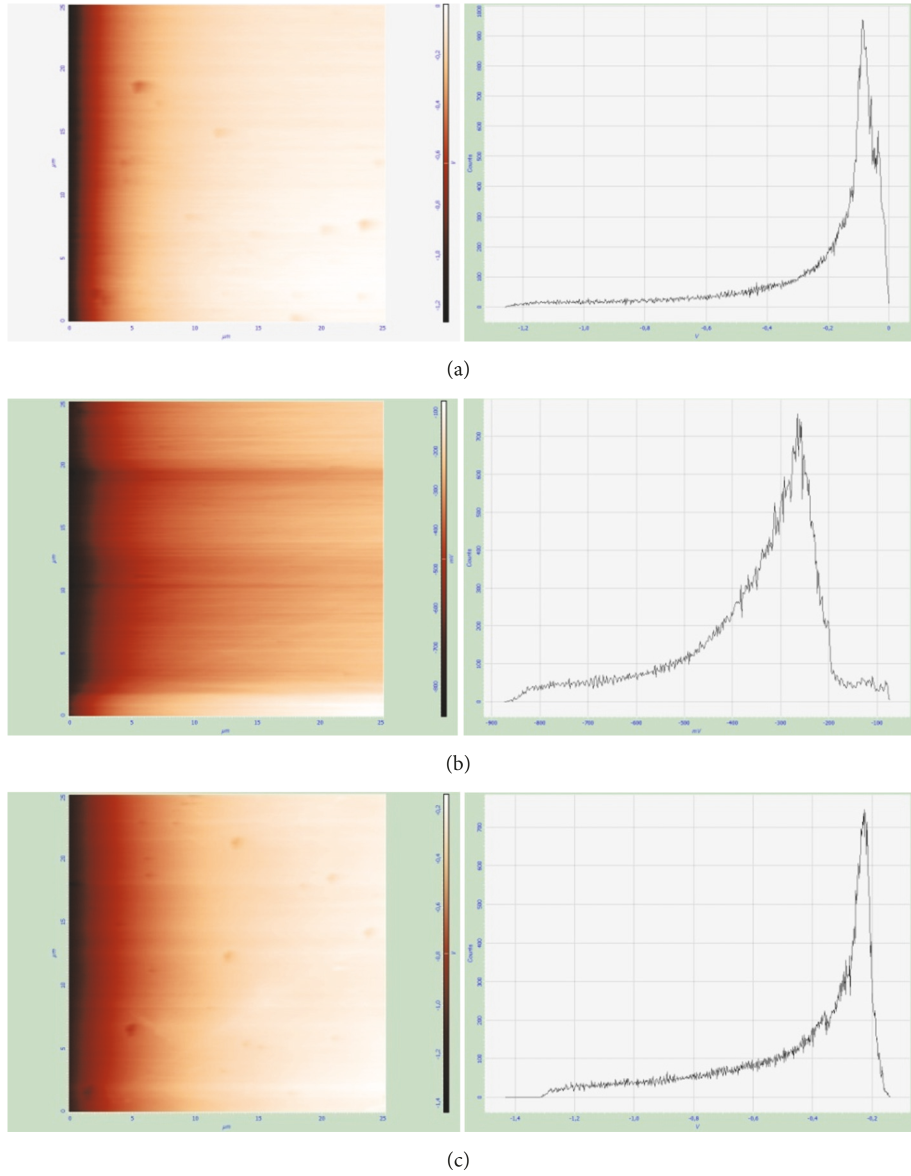

FIGURE 4: KPFM topography (left) and CP histogram analysis (right) for S1, S2, and S3 samples.

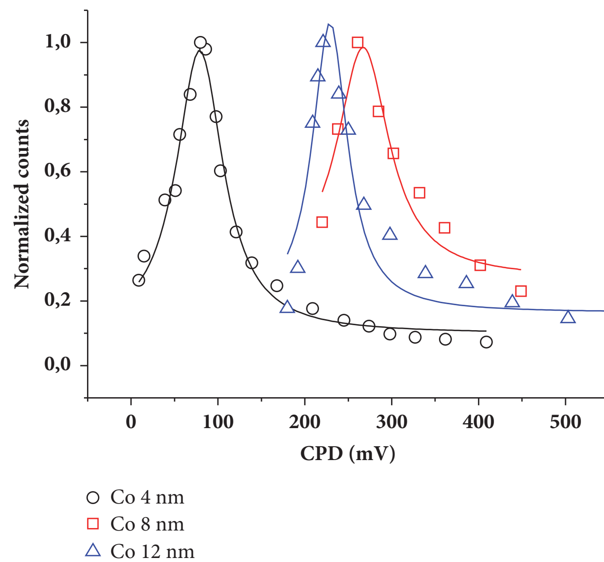

FIGURE 5: CP histogram fits for different interlayer thickness. The continuous line is the fit result.

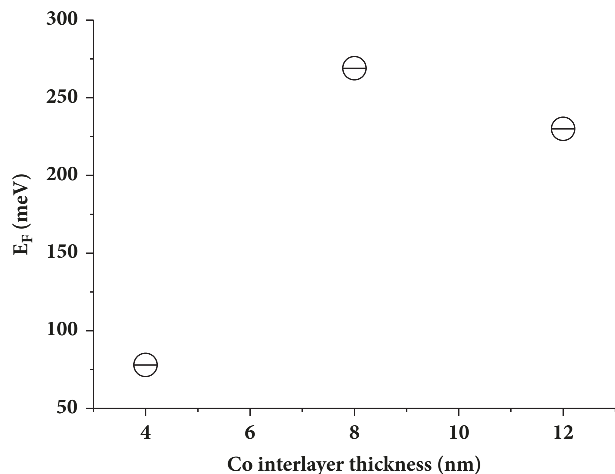

Figure 6: Fermi level versus Co interlayer thickness.

Disclosure

Marcos Meyer and Laura C. Damonte are members of CONICET.

Conflicts of Interest

The authors declare that they have no conflicts of interest.

Acknowledgments

This work was supported by Consejo Nacional de Investigaciones Científicas (CONICET), Argentina (PIP 112-201101-00313).

References

[1] A. Stadler, "Transparent conducting oxides—an up-to-date overview," *Materials* , vol. 5, no. 12, pp. 661–683, 2012.

[2] M. D. Tolosa, L. C. Damonte, H. Brine, H. J. Bolink, and M. A. Hernández-Fenollosa, "Nucleant layer effect on nanocolumnar ZnO films grown by electrodeposition," *Nanoscale Research Letters*, vol. 8, no. 1, p. 135, 2013.

[3] P. C. Lansåker, P. Petersson, G. A. Niklasson, and C. G. Granqvist, "Thin sputter deposited gold films on In2O3:Sn, SnO2:In, TiO2 and glass: Optical, electrical and structural effects," *Solar Energy Materials & Solar Cells*, vol. 117, pp. 462–470, 2013.

[4] K. Ellmer, "Past achievements and future challenges in the development of optically transparent electrodes," *Nature Photonics*, vol. 6, no. 12, pp. 809–817, 2012.

[5] H. Liu, V. Avrutin, N. Izyumskaya, Ü. Özgr, and H. Morkoç, "Transparent conducting oxides for electrode applications in light emitting and absorbing devices," *Superlattices and Microstructures*, vol. 48, no. 5, pp. 458–484, 2010.

[6] Y.-S. Park, H.-K. Kim, and S.-W. Kim, "Thin Ag layer inserted GZO multilayer grown by roll-to-roll sputtering for flexible and transparent conducting electrodes," *Journal of The Electrochemical Society*, vol. 157, no. 8, pp. J301–J306, 2010.

[7] A. Dhar and T. L. Alford, "High quality transparent TiO2/Ag/TiO2 composite electrode films deposited on flexible substrate at room temperature by sputtering," *APL Materials*, vol. 1, no. 1, Article ID 012102, 2013.

[8] A. Dhar and T. L. Alford, "Optimization of Nb_2O_5/Ag/Nb_2O_5 multilayers as transparent composite electrode on flexible substrate with high figure of merit," *Journal of Applied Physics*, vol. 112, no. 10, Article ID 103113, 2012.

[9] C. Guillén and J. Herrero, "TCO/metal/TCO structures for energy and flexible electronics," *Thin Solid Films*, vol. 520, no. 1, pp. 1–17, 2011.

[10] D. Zhang, H. Yabe, E. Akita, P. Wang, R.-I. Murakami, and X. Song, "Effect of silver evolution on conductivity and transmittance of ZnO/Ag thin films," *Journal of Applied Physics*, vol. 109, no. 10, Article ID 104318, 2011.

[11] V. Bhosle, A. Tiwari, and J. Narayan, "Metallic conductivity and metal-semiconductor transition in Ga-doped ZnO," *Applied Physics Letters*, vol. 88, no. 3, Article ID 032106, pp. 1–3, 2006.

[12] H.-T. Sun, X.-P. Wang, Z.-Q. Kou, L.-J. Wang, J.-Y. Wang, and Y.-Q. Sun, "Optimization of TiO2/Cu/TiO2 multilayers as a transparent composite electrode deposited by electron-beam evaporation at room temperature," *Chinese Physics B*, vol. 24, no. 4, Article ID 047701, 2015.

[13] A. Dhar and T. L. Alford, "Optimization of TiO2/Cu/TiO2 multilayer as transparent composite electrode (TCE) deposited on flexible substrate at room temperature," *ECS Solid State Letters (SSL)*, vol. 3, no. 11, pp. N33–N36, 2014.

[14] J. H. Kim, H.-K. Lee, J.-Y. Na, S.-K. Kim, Y.-Z. Yoo, and T.-Y. Seong, "Dependence of optical and electrical properties on Ag thickness in TiO2/Ag/TiO2 multilayer films for photovoltaic devices," *Ceramics International*, vol. 41, no. 6, pp. 8059–8063, 2015.

[15] S. Kumar and S. Singh, "Effect & Growth of TiO_2 Thin Films for Solar Cell Applications," *International Journal of Hybrid Information Technology*, vol. 9, no. 2, pp. 267–274, 2016.

[16] D. Hocine, M. S. Belkaid, M. Pasquinelli et al., "Improved efficiency of multicrystalline silicon solar cells by TiO 2 antireflection coatings derived by APCVD process," *Materials Science in Semiconductor Processing*, vol. 16, no. 1, pp. 113–117, 2013.

[17] G. Helsch and J. Deubener, "Compatibility of antireflective coatings on glass for solar applications with photocatalytic properties," *Solar Energy*, vol. 86, no. 3, pp. 831–836, 2012.

[18] S. Zhang, S. Zhang, B. Peng et al., "High performance hydrogenated TiO2 nanorod arrays as a photoelectrochemical sensor for organic compounds under visible light," *Electrochemistry Communications*, vol. 40, pp. 24–27, 2014.

[19] X. Yang, C. Cao, L. Erickson, K. Hohn, R. Maghirang, and K. Klabunde, "Synthesis of visible-light-active TiO2-based photocatalysts by carbon and nitrogen doping," *Journal of Catalysis*, vol. 260, no. 1, pp. 128–133, 2008.

[20] J. Moon, J.-A. Park, S.-J. Lee, T. Zyung, and I.-D. Kim, "Pd-doped TiO2 nanofiber networks for gas sensor applications," *Sensors and Actuators B: Chemical*, vol. 149, no. 1, pp. 301–305, 2010.

[21] J. Moon, H.-P. Hedman, M. Kemell et al., "A study of monitoring hydrogen using mesoporous TiO2 synthesized by anodization," *Sensors and Actuators B: Chemical*, vol. 189, pp. 246–250, 2013.

[22] Z. Wen and L. Tian-mo, "Gas-sensing properties of SnO2-TiO2-based sensor for volatile organic compound gas and its sensing mechanism," *Physica B: Condensed Matter*, vol. 405, no. 5, pp. 1345–1348, 2010.

[23] H. Chen, Y. Liu, C. Xie, J. Wu, D. Zeng, and Y. Liao, "A comparative study on UV light activated porous TiO2 and ZnO film

sensors for gas sensing at room temperature," *Ceramics International*, vol. 38, no. 1, pp. 503–509, 2012.

[24] T. Xie, N. Sullivan, K. Steffens et al., "UV-assisted room-temperature chemiresistive NO_2 sensor based on TiO_2 thin film," *Journal of Alloys and Compounds*, vol. 653, Article ID 35296, pp. 255–259, 2015.

[25] K. F. Albertin, M. A. Valle, and I. Pereyra, "Study of MOS capacitors with TiO2 and SiO2/TiO2 gate dielectric," *Journal of Integrated Circuits and Systems*, vol. 2, no. 2, pp. 89–93, 2007.

[26] Y.-F. Tian, S.-J. Hu, S.-S. Yan, and L.-M. Mei, "Oxide magnetic semiconductors: Materials, properties, and devices," *Chinese Physics B*, vol. 22, no. 8, Article ID 088505, 2013.

[27] R. Chau, B. Doyle, S. Datta, J. Kavalieros, and K. Zhang, "Integrated nanoelectronics for the future," *Nature Materials*, vol. 6, no. 11, pp. 810–812, 2007.

[28] N. H. Hong, J. Sakai, N. Poirot, and V. Brize, "Room-temperature ferromagnetism observed in undoped semiconducting and insulating oxide thin films," *Physical Review B*, vol. 73, Article ID 132404, 2006.

[29] Md. Abdullah Al Asad, Md. Omar Faruk, Md. Faruk Hossain, and Md. Saiful Islam, "Analysis the Optical Properties of Co, TiO2 and Co/TiO2 Multilayer Thin Films of Different Thickness Deposited By E-Beam Technique," *Journal of Applied Physics*, vol. 7, no. 4, pp. 64–69, 2015.

[30] Y. Yang, Q. Zhang, B. Zhang et al., "The influence of metal interlayers on the structural and optical properties of nano-crystalline TiO 2 films," *Applied Surface Science*, vol. 258, no. 10, pp. 4532–4537, 2012.

[31] T. Su and H.-F. Zhang, "Influence of oxygen partial pressure on the Fermi level of Zno films investigated by Kelvin probe force microscopy," *Chinese Physics Letters*, vol. 29, no. 12, 2012.

[32] Y. Zhang, D. J. Hellebusch, N. D. Bronstein et al., "Ultrasensitive photodetectors exploiting electrostatic trapping and percolation transport," *Nature Communications*, vol. 7, Article ID 11924, 2016.

[33] M. Nonnenmacher, M. P. O'Boyle, and H. K. Wickramasinghe, "Kelvin probe force microscopy," *Applied Physics Letters*, vol. 58, no. 25, pp. 2921–2923, 1991.

[34] A. J. Weymouth and F. J. Giessibl, "The effect of sample resistivity on Kelvin probe force microscopy," *Applied Physics Letters*, vol. 101, no. 21, Article ID 213105, 2012.

[35] O. Tal, W. Gao, C. K. Chan, A. Kahn, and Y. Rosenwaks, "Measurement of interface potential change and space charge region across metal/organic/metal structures using Kelvin probe force microscopy," *Applied Physics Letters*, vol. 85, no. 18, pp. 4148–4150, 2004.

[36] B.-Y. Tsui, C.-M. Hsieh, P.-C. Su, S.-D. Tzeng, and S. Gwo, "Two-dimensional carrier profiling by kelvin-probe force microscopy," *Japanese Journal of Applied Physics*, vol. 47, no. 6, pp. 4448–4453, 2008.

[37] K. Lau, Y. Liu, Q. Li, Z. Li, R. L. Withers, and Z. Xu, "Surface Characterisation of a Ferroelectric Single Crystal by Kelvin Probe Force Microscopy," *Journal of Surface Engineered Materials and Advanced Technology*, vol. 03, no. 03, pp. 190–194, 2013.

[38] S. Sadewasser, P. Jelinek, C.-K. Fang et al., "New insights on atomic-resolution frequency-modulation Kelvin-probe force-microscopy imaging of semiconductors," *Physical Review Letters*, vol. 103, no. 26, Article ID 266103, 2009.

[39] W. Melitz, J. Shen, A. C. Kummel, and S. Lee, "Kelvin probe force microscopy and its application," *Surface Science Reports*, vol. 66, no. 1, pp. 1–27, 2011.

[40] H. Schmidt, S. Habicht, S. Feste, A.-D. Müller, and O. G. Schmidt, "Kelvin probe force microscopy for characterizing doped semiconductors for future sensor applications in nano- and biotechnology," *Applied Surface Science*, vol. 281, pp. 24–29, 2013.

[41] C. Barth, A. S. Foster, C. R. Henry, and A. L. Shluger, "Recent trends in surface characterization and chemistry with high-resolution scanning force methods," *Advanced Materials*, vol. 23, no. 4, pp. 477–501, 2011.

[42] C. Leung, D. Maradan, A. Kramer, S. Howorka, P. Mesquida, and B. W. Hoogenboom, "Improved Kelvin probe force microscopy for imaging individual DNA molecules on insulating surfaces," *Applied Physics Letters*, vol. 97, no. 20, Article ID 203703, 2010.

[43] P. Gao and Y. Cai, "Label-free detection of the aptamer binding on protein patterns using Kelvin probe force microscopy (KPFM)," *Analytical and Bioanalytical Chemistry*, vol. 394, no. 1, pp. 207–214, 2009.

[44] H. O. Jacobs, H. F. Knapp, S. Müller, and A. Stemmer, "Surface potential mapping: A qualitative material contrast in SPM," *Ultramicroscopy*, vol. 69, no. 1, pp. 39–49, 1997.

[45] S. Sadewasser and T. Glatzel, "Kelvin probe force microscopy," *Springer Series in Surface Sciences*, vol. 48, no. 1, 2012.

[46] P. Girard and A. N. Titkov, "Electrostatic force and force gradient microscopy: principles, points of interest and application to characterisation of semiconductor materials and devices," in *Applied Scanning Probe Methods II: Scanning Probe Microscopy Techniques*, B. Bhushan and H. Fuchs, Eds., NanoScience and Technology, pp. 283–320, Springer, Berlin, Germany, 2006.

[47] K. Sivaramakrishnan and T. L. Alford, "Metallic conductivity and the role of copper in ZnO/Cu/ZnO thin films for flexible electronics," *Applied Physics Letters*, vol. 94, no. 5, Article ID 052104, 2009.

[48] H. Han, J. W. Mayer, and T. L. Alford, "Band gap shift in the indium-tin-oxide films on polyethylene napthalate after thermal annealing in air," *Journal of Applied Physics*, vol. 100, no. 8, Article ID 083715, 2006.

[49] J. Tauc, R. Grigorovic, and A. Vancu, "Optical properties and electronic structure of amorphous germanium," *Physica Status Solidi B*, vol. 15, no. 2, pp. 627–637, 1966.

[50] E. A. Davis and N. F. Mott, "Conduction in non-crystalline systems conductivity, optical absorption and photoconductivity in amorphous semiconductors," *Philosophical Magazine*, vol. 22, no. 179, pp. 903–922, 1970.

[51] A. Klein, C. Körber, A. Wachau et al., "Transparent conducting oxides for photovoltaics: Manipulation of fermi level,work function and energy band alignment," *Materials* , vol. 3, no. 11, pp. 4892–4914, 2010.

[52] H. Shin, B. Lee, C. Kim et al., "Measurement and visualization of doping profile in silicon using Kelvin probe force microscopy (KPFM)," *Electronic Materials Letters*, vol. 1, p. 127, 2005.

[53] S. Barbet, R. Aubry, M. di Forte-Poisson et al., "Surface potential of n- and p-type GaN measured by Kelvin force microscopy," *Applied Physics Letters*, vol. 93, no. 21, p. 212107, 2008.

[54] S. Dixit, A. Srivastava, R. K. Shukla, and A. Srivastava, "Pulsed laser deposited ZnO films and their humidity sensing behavior," *Journal of Materials Science: Materials in Electronics*, vol. 19, no. 8-9, pp. 788–792, 2008.

[55] R. Huang, S. Ye, K. Sun, K. S. Kiang, and C. H. K. de Groot, "Fermi Level Tuning of ZnO Films Through Supercycled Atomic Layer Deposition," *Nanoscale Research Letters*, vol. 12, article no. 541, 2017.

[56] L. Peres, A. Bou, C. Cornille, D. Barakel, and P. Torchio, "Work function measurement of multilayer electrodes using Kelvin probe force microscopy," *Journal of Physics D: Applied Physics*, vol. 50, no. 13, Article ID 13LT01, 2017.

[57] P. Narchi, V. Neplokh, V. Piazza et al., "Surface potential investigation on interdigitated back contact solar cells by Scanning Electron Microscopy and Kelvin Probe Force Microscopy: Effect of electrical bias," *Solar Energy Materials & Solar Cells*, vol. 161, pp. 263–269, 2017.

[58] C. K. Boumenou, Z. N. Urgessa, S. R. T. Djiokap, J. R. Botha, and J. Nel, "Effect of dopant density on contact potential difference across n-type GaAs homojunctions using Kelvin Probe Force Microscopy," *Physica B: Condensed Matter*, 2017.

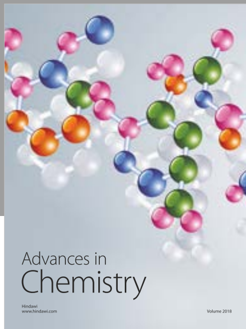

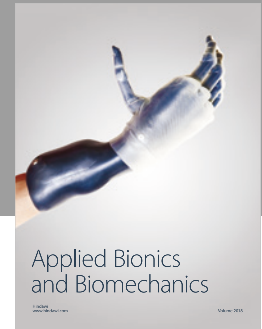

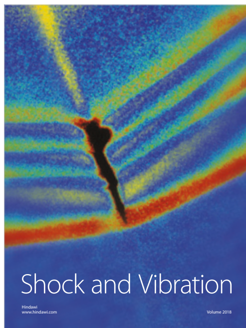

Hindawi

Submit your manuscripts at
www.hindawi.com